Structure of elongated and spherulitic domains in long pitch cholesterics with homeotropic boundary alignment

A.E. Stieb

▶ **To cite this version:**

A.E. Stieb. Structure of elongated and spherulitic domains in long pitch cholesterics with homeotropic boundary alignment. Journal de Physique, 1980, 41 (9), pp.961-969. 10.1051/jphys:01980004109096100 . jpa-00208928

HAL Id: jpa-00208928
https://hal.science/jpa-00208928

Submitted on 4 Feb 2008

HAL is a multi-disciplinary open access archive for the deposit and dissemination of scientific research documents, whether they are published or not. The documents may come from teaching and research institutions in France or abroad, or from public or private research centers.

L'archive ouverte pluridisciplinaire **HAL**, est destinée au dépôt et à la diffusion de documents scientifiques de niveau recherche, publiés ou non, émanant des établissements d'enseignement et de recherche français ou étrangers, des laboratoires publics ou privés.

J. Physique **41** (1980) 961-969 SEPTEMBRE **1980**, PAGE 961

Classification
Physics Abstracts
61.30

Structure of elongated and spherulitic domains in long pitch cholesterics with homeotropic boundary alignment (*)

A. E. Stieb

Fraunhofer-Institut für Angewandte Festkörperphysik, Eckerstr. 4, 7800 Freiburg, W. Germany

(*Reçu le 3 décembre 1979, accepté le 12 mai 1980*)

Résumé. — Les domaines allongés ou sphériques observés dans les couches cholestériques, dont la période est comparable à l'épaisseur de la lame, sont étudiés par des méthodes optiques. De nouvelles propriétés et trois différentes variétés de domaines ont été trouvées. L'orientation perpendiculaire à la surface et toutes les propriétés connues des domaines ont été considérées en construisant leur champ directeur. La ligne verticale de disclination du centre des domaines sphériques est découverte comme étant une singularité métastable.

Abstract. — Elongated and spherulitic domains, as occurring in cholesteric layers with a pitch equal to about a layer spacing, have been investigated by optical methods. Several new properties have been discovered, and three varieties of domains could be distinguished. All properties of the domains, known up to now, and the homeotropic boundary alignment have been taken into account to construct their director field. The vertical defect line in the centre of the spherulitic bubble domains has been discovered to be a metastable singularity.

1. **Introduction.** — When a cholesteric liquid crystal, or a nematic liquid crystal with a chiral solute, is placed between two lecithin coated glass plates, the whole layer is homeotropically aligned if the genuine pitch p_0 of the liquid crystal is large compared to the layer spacing d. The liquid crystal is then kept under an elastic torque strain by the alignment at the boundary plates, and the density of the elastic free energy G per area A is

$$G/A = 2\,\pi^2\,K_2\,d/p_0^2 \qquad (1)$$

where K_2 is the Frank elastic constant for twist [1]. The energy increases with decreasing pitch until a more favourable conical deformation replaces the homeotropic alignment. This is the case for the critical thickness [2]

$$d_c = \tfrac{1}{2}\,p_0\,K_3/K_2 \qquad (2)$$

of the layer, where K_3 is the Frank elastic constant for bend [1]. The homogeneous conical deformation is not stable; it is slowly replaced by partly ordered domain stripes, resembling the fingerprint patterns [3]. For layer spacings larger than $2\,d_c$, more complicated types of deformation are observed. In this paper the fingerprint domain and spherulitic bubble textures [4, 5, 6] as occurring in the regime of $d_c < d < 2\,d_c$ are investigated.

Several researchers have tried to evaluate the structure of the cholesteric domains and have given models of their director field. The fingerprint patterns described by Cladis and Kléman [7] had been observed in rather thick layers with weak or no homeotropic boundary anchoring. Therefore the cholesteric liquid crystal was nearly free to align in its natural helical structure. The observed pattern of white and black stripes had a periodicity of about $p_0/2$. By a slight disturbance of the layer the helical axis was reoriented from a parallel to a perpendicular direction to the glass plates [7], which indicates the weak surface anchoring. No singular disclination lines along the edges of the domain stripes at the glass plates, as postulated by the authors, were detected.

In the following, Kashnow *et al.* [8] have described a nucleation process for cholesteric domains, also assuming disclinations near to the glass surfaces. Akahane and Tako have extended the defect model to the spherulitic domains [9]. However, it can be objected to these models that the deformation range about the postulated disclinations would have the same order of magnitude as the whole domain itself, so that their influence cannot be neglected. Bhide

(*) Presented at the 3. Liquid Crystal Conf., Budapest 1979; This work was partly carried out in the Dep. of Chemistry, Temple University, Philadelphia.

Article published online by EDP Sciences and available at http://dx.doi.org/10.1051/jphys:01980004109096100

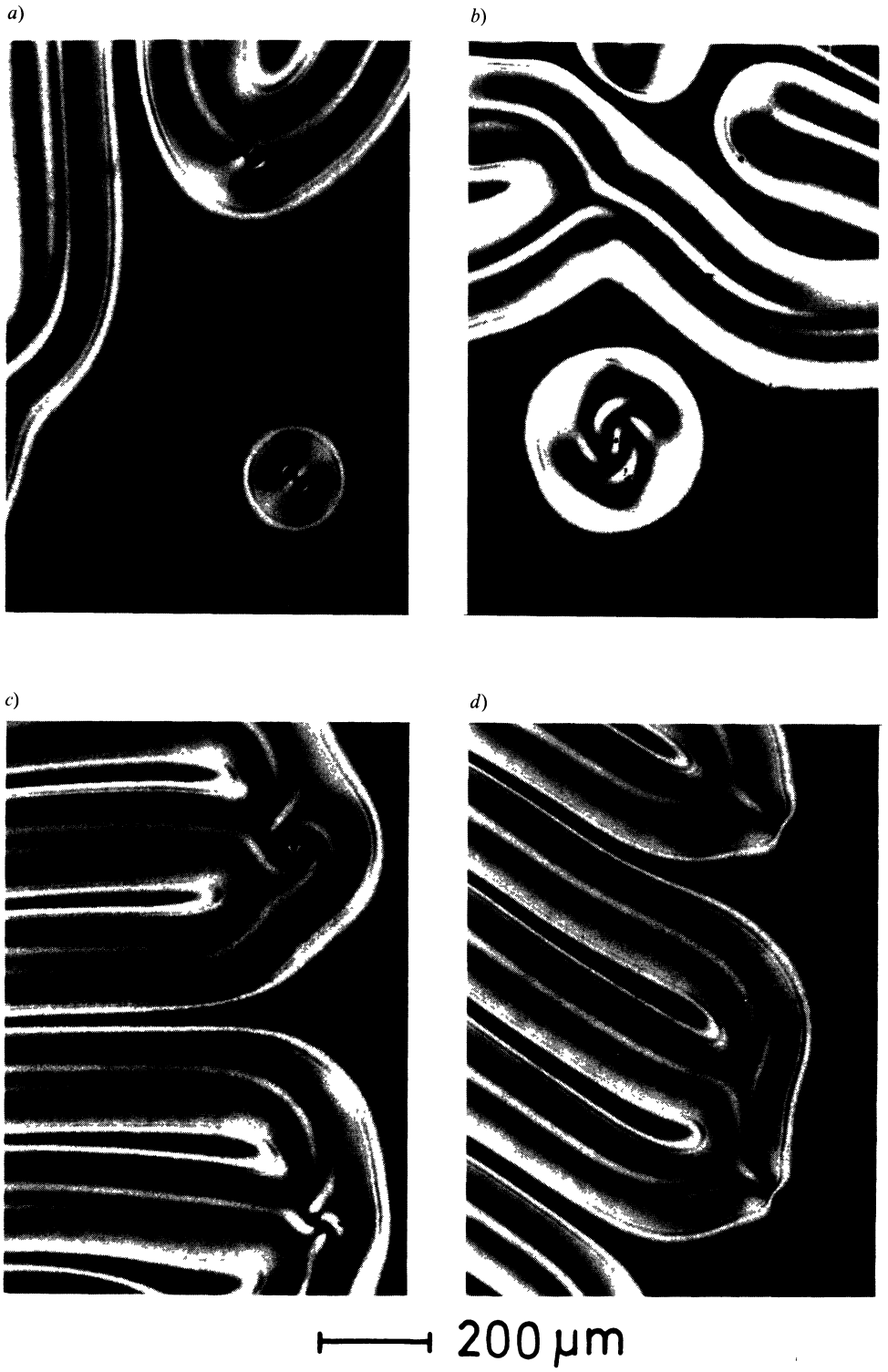

Fig. 1. — Different types of cholesteric domains in a layer with a small wedge angle, homeotropic boundary alignment and $d < p_0$ (mixture of MBBA/EBBA with menthol, crossed polarizers); *a*) Spherulitic and extended bubble domains each containing a vertical defect line; *b*) Circular loop domain, enclosing a residual homeotropic area ; *c*) Loop domains and *d*) Polar domains in the extended and branched state.

et al. [10] as well as Adamczyk ([1]) have even postulated a phase separation of a chiral nematic liquid crystal into cholesteric droplets suspended in a nematic matrix. Press and Arrott [11] have been the first to construct a cross section of the fingerprint domains, respecting both, the smooth structure and the homeotropic boundary alignment of the cholesteric layer.

If layers with strong homeotropic boundary anchoring and a spacing of about $d = d_c$ are used, the fingerprint texture is forced into a characteristic domain pattern, exhibiting interference fringes due to the double refraction profile. The observed properties of the elongated and spherulitic domains are then similar for all layers with the same ratio of d/p_0. Therefore the topological structure of the domains seems to be well defined, while the fine structure of the director field depends on the relative magnitudes of the elastic constants.

In this paper, these common properties are taken into consideration, to complete the model by Press and Arrott and to propose a new model for the spherulitic domains.

2. **Properties of the domains.** — At first, three different varieties of domains, each of which can exist either in a bubble form or in the extended stripe form, are to be distinguished. The spherulitic bubble domain with a central *defect* and the corresponding stripe domain are shown in figure 1*a*. At the bottom of figure 1*b*, a *looped* stripe domain is to be seen in a state where the enclosed homeotropic area is nearly contracted to a point, while in figure 1*c* branched loop domains are shown. There is also existing a *polar* type of domain [12, 13], which is shown in its extended and branched form in figure 1*d*. Common to the three domain types is the structure of their extended stripes and of at least one of their ends, which is identical with the outer parts of the spherulitic bubble domain. The other end in the polar domains is more peaked and its pattern of fringes differs from that of the round ends. Each domain system without a loop or a defect has been found to exhibit one end of that kind. There has been observed a continuous transition from a loop domain to a polar domain, analogous to the sequence of the figure 1*c* (top), 1*c* (bottom) and 1*d*.

No singular lines parallel to the glass plates could be detected in these domains; only the vertical defect line in the centre of the spherulitic domains was found. Even the branching of a domain and the ends left after an intersection of a domain have a continuous structure. The spherulitic bubble and the unbranched loop domains, both have a rotational symmetry about the vertical axis, since the pattern of the black bands is not changed by a rotation of the specimen on the stage of the polarizing microscope. A loop domain, instead of forming polar ends after contraction, can also be converted into a spherulite under the influence of an electric field reinforcing the homeotropic alignment [14]. The symmetry of the black band pattern, displayed by the domain between crossed polarizers, is changed by this conversion process (compare Figs. 1*a* and *b*).

If $d < 2\,d_c$, the domain stripes are separated from each other by a narrow homeotropic transition region [11, 14]. Only the peaked ends of the polar domains are attracted by and merging with all other parts of the domains (see Fig. 2). By this merging

([1]) 3. Liquid Crystal Conf., Budapest (1979).

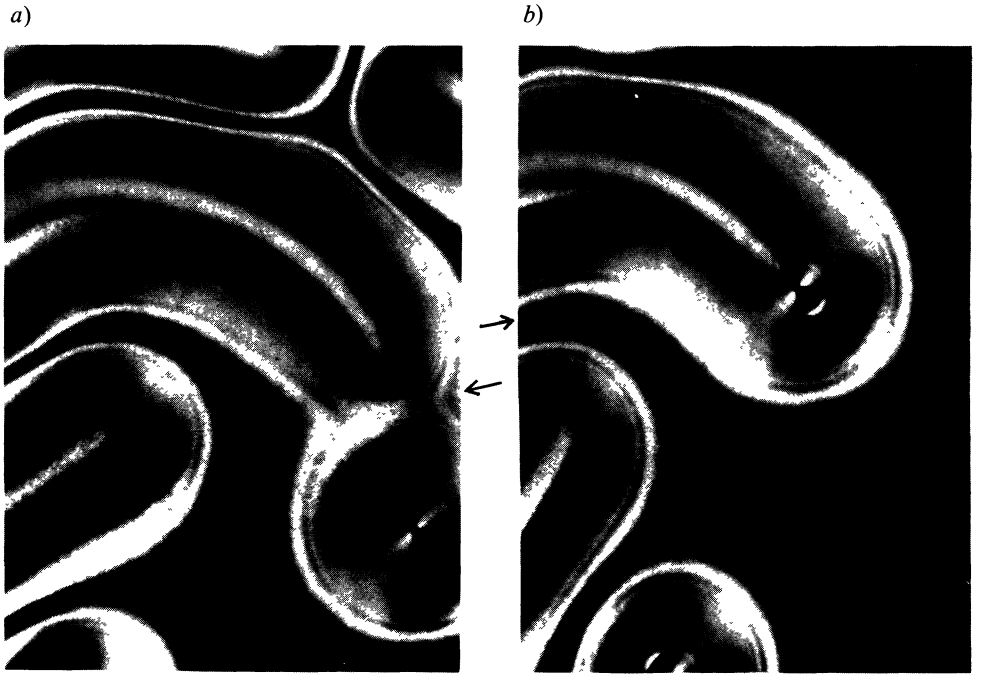

Fig. 2. — Attraction (*a*) and merging (*b*) of a polar domain and a spherulitic domain by annihilation of their opposite twist deformations in the outer parts of their structure.

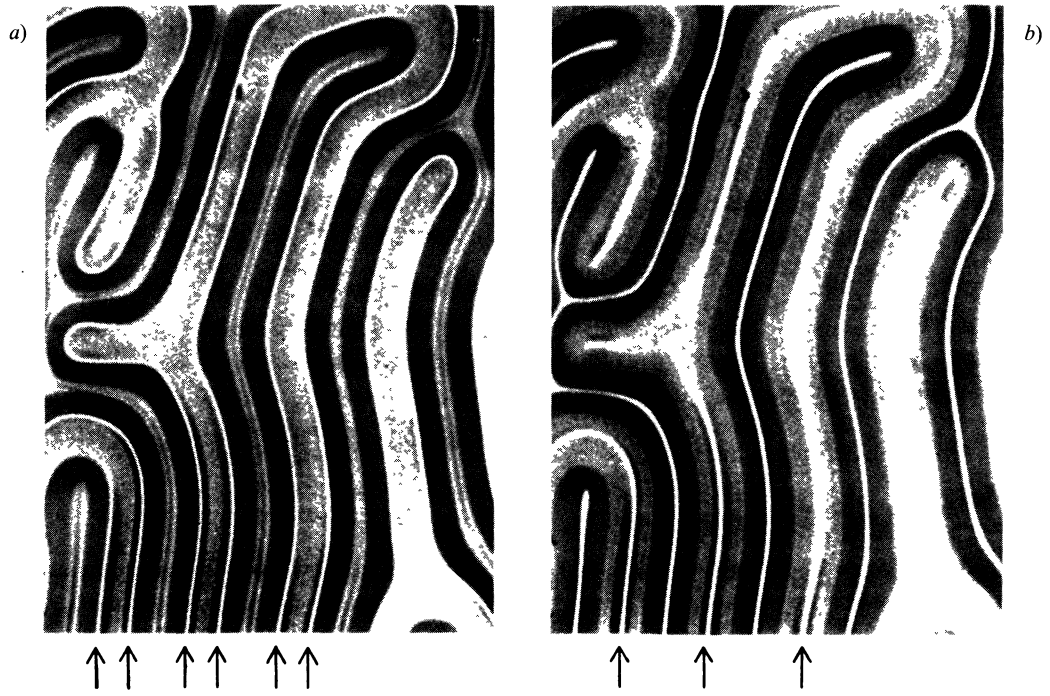

Fig. 3. — Focal lines (↑) of the elongated domains in unpolarized light if the microscope is focussed to a plane above (*a*) and below (*b*) the liquid crystal layer.

process or by growing, domain systems are created which are branched in such a way that only the number of the round ends is increased. Never a branching to the other side and more than one end of the peaked type have been observed in a domain system.

In the domain stripes a focussing effect can be observed which is due to the double refraction distribution. A pair of focal lines with a direction parallel to the edges of the domain is seen if the microscope is focussed to a plane above the layer (arrows in figure 3*a*). Focussing to below the liquid crystal layer shows a single focal line as if produced by a concave cylinder lens in the centre of the domain. More accurately, the double refraction profile has been traced by measuring the distribution of the fringes, as they are to be seen, for example, in figure 2. These data are used to test the proposed model of the domain structure (see next paragraph and figure 7).

If the spherulitic domains are observed in light, which is polarized either before or after passing the specimen, the patterns of the black brushes are not the same, but have an opposite spiral sense (see Fig. 4). By rotating the polarizer, the pattern is rotated syn-

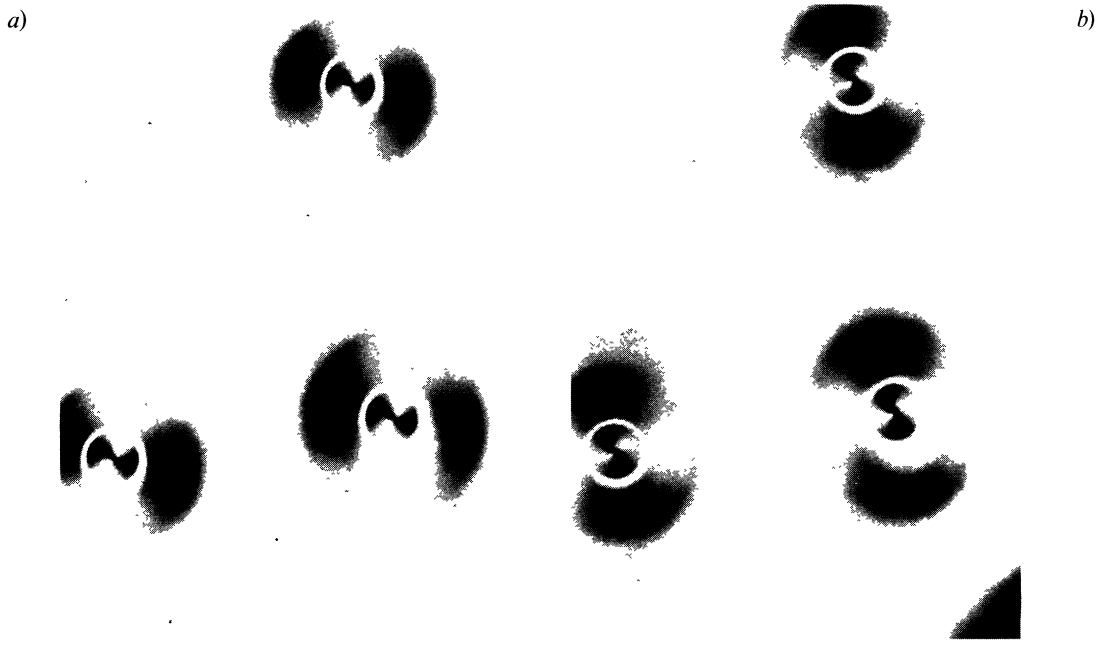

Fig. 4. — Spherulitic bubble domains in (*a*) polarized light (↔) and (*b*) analysed light (↕). The two patterns have opposite spiral senses and their superposition yields a similar pattern as that of a spherulite between crossed polarizers.

chronously without further change. A bright focal ring around the centre of the domain can be seen if the microscope is focussed somewhat to above the liquid crystal layer. It corresponds to the pair of focal lines in the domain stripes, at the round ends of which the lines are closed to a semi-circle. This effect indicates that the effective refractive index increases from the border to the centre of the spherulite where it possibly decreases again slightly so that a ring-shaped convex lens is formed. In some cases, however a stronger decrease in the centre, indicated by interference fringes, has been observed.

In figure 5 an array of bubble domains is to be seen, which has been generated using the *dynamic scattering*

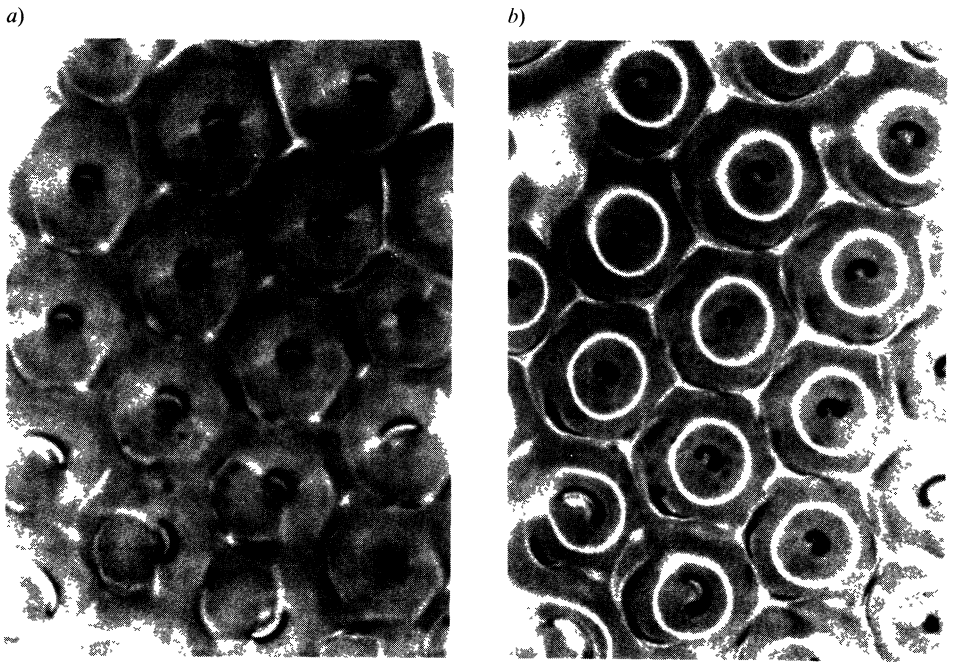

Fig. 5. — Array of spherulitic domains, generated by the dynamic scattering effect. After a slight shift of one glass plate, the central black points are detected to be vertical defect lines. The microscope is focussed to the lower (*a*) and the upper (*b*) boundary of the liquid crystal layer, where the lines are attached to the glass plates.

effect [5]. After the glass plates have been sheared slightly, the central defect line of the spherulites can be seen clearly. It is attached to both glass plates, as focussing to the upper and the lower boundary of the layer reveals. If an electric field reinforcing the homeotropic alignment is increased, the spherulites shrink to a critical diameter and suddenly disappear without leaving back a trace, especially no singular disclination lines or points. If the field is again lowered, a pronounced hysteresis effect is observed : the nucleation of new spherulites is strongly hindered and small dust particles become the nucleation sites.

3. **Structure of the elongated domains.** — The cross section of an elongated domain, as given by Press and Arrott [11], is in qualitative agreement with the experimental observations. Using a similar cross section, the structure of a looped elongated domain is sketched in figure 6.

This structure has the required rotational symmetry about its central vertical axis, where a residual area of homeotropic alignment is left. The midplane across the loop domain (upper part of figure 6) is no mirror plane, nor the vertical cross section across the centre (lower part of figure 6). The deformation along a vertical axis is essentially conical, and the twist sense is everywhere the same as determined by the cholesteric helix.

Caused by an external force, continuous generation and annihilation of the singularity-free polar and loop domains can take place *via* a synchronous change of the overall twist and tilt angle. This continuous change of twist is allowed because the helical axis and the director of the liquid crystal layer are parallel to each other at the glass surfaces. The maximum tilt angle of the director in the midplane of the layer seems to be dependent on d/p_0 and on the relative magnitudes of the elastic constants. In the Press and Arrott model for identical elastic constants the maximum tilt angle was about 90°. In the experiments, however, a small decrease of the effective refractive index is usually observed in the centre of the domain. This is demonstrated by the concave lens effect as shown in figure 3, and has also been reported by Akahane, Nakao and Tako [15]. Therefore we have to suppose a maximum midplane tilt angle of more than 90° in the centre of the stripe domain. In order to find this maximum tilt angle, the distribution of the double refraction fringes in monochromatic light has been measured across a domain (small circles in figure 7*a*). In the following, the director field model, sketched in figure 6, is expressed by an empirical function with fit parameters. The

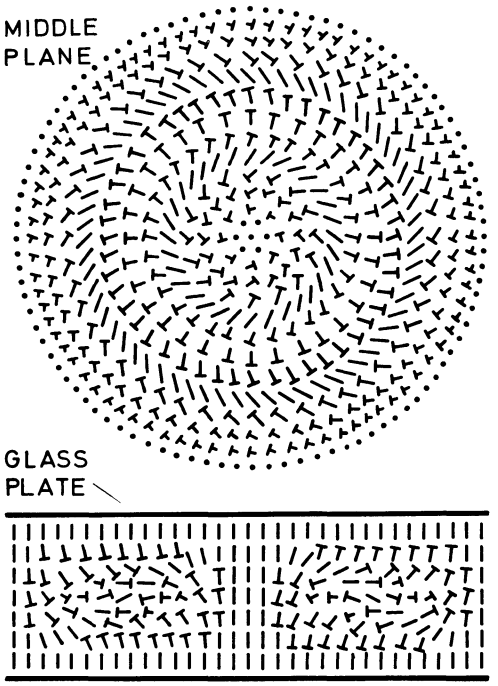

Fig. 6. — Director field cross sections of a singularity-free loop domain, seen from the top and from the side. The bars, *nails*, and dots indicate the direction of the local optical axis (director) in the liquid crystal as parallel, tilted, and perpendicular to the figure plane, respectively. The sense of twist is the same over the whole structure. A continuous annihilation process of the domain can take place *via* a continuous decrease of the midplane tilt angle synchronously with an untwisting about the vertical axis.

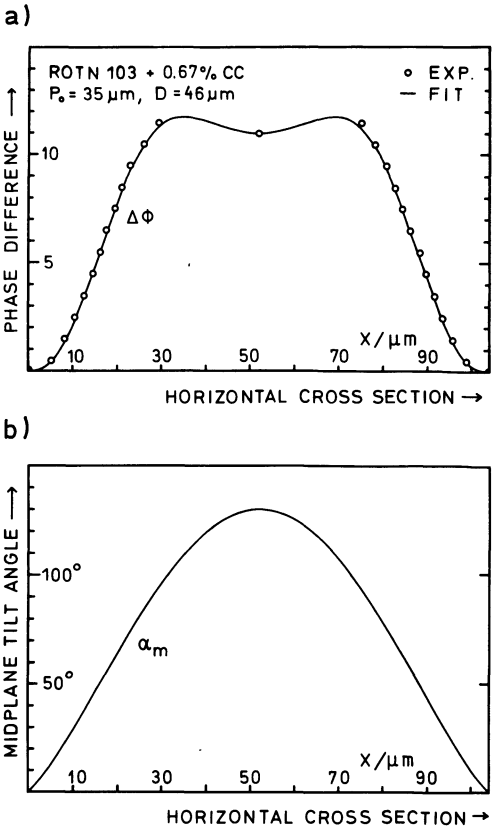

Fig. 7. — Distribution of the double refraction phase difference across a cholesteric domain stripe with a maximum midplane tilt angle of 130° (λ = 544 nm); *a*) Distribution of the black fringes across a domain (exp. values : ○, centre of the domain : bright) and approximated optical phase difference function $\Delta\varphi$ (solid line); *b*) Midplane tilt angle α_m across a stripe domain, as received by the approximation of the experimental $\Delta\varphi$ values.

optical retardation function, calculated from this model, is finally fitted to the experimental values.

The conical twist along the z-coordinate (perpendicular to the glass plates) is represented by a director rotating on an opening and reclosing cone with a vertical axis and with a maximum aperture of 2 α_m, the double tilt angle in the midplane of the layer. In our model, the tilt angle α of the optical axis is varying sinusoidally between the glass plates :

$$\alpha = \alpha_m \cdot \sin(\pi z/d) . \tag{3}$$

The midplane tilt angle α_m is changing periodically in the x-direction perpendicular to the domain stripes. Here it is approximated by

$$\alpha_m = \alpha_{mm} \cdot \sin^a(\pi x/b) \tag{4}$$

where b is the width of the domain, and where the maximum midplane tilt angle α_{mm} and the power a are fit parameters. The rotation of the director on the cone must not further be specified if only the optical retardation is calculated for a pitch large compared to the wavelength of light [16].

The optical retardation is then given by

$$\Delta\varphi(x) = (n_e - n_0)\frac{1}{\lambda}\int_0^d [\sin^2(\alpha_m(x) \cdot \sin(\pi z/d))]\, dz \tag{5}$$

where n_e and n_0 are the extraordinary and ordinary refractive indices, respectively, and λ the wavelength of the light.

The integral (5) must be evaluated for all values of x. It has minima at the edges of the domain and a flat minimum in the centre at $x = b/2$. Between the minima two maxima are found. The approximation to the experimental values is carried out by varying the fit parameters a and α_{mm}, while b and $(n_e - n_0)\, d/\lambda$ are measured. For a mixture of ROTN 103 (Roche) with 0.67 % cholesteryl-chloride (CC), the values at room temperature have been a = 1.24, α_{mm} = 130°, and $(n_e - n_0)\, d/\lambda$ = 16.8. Of course, these values are strongly dependent on the material parameters. The fit curve of the optical retardation, as shown in figure 7*a*, is in good agreement with the characteristic experimental distribution, given by the small circles. The function of the midplane tilt angle α_m across a domain is shown in figure 7*b* for the respective fit parameters.

Press and Arrott have only calculated the cross section of infinitely elongated fingerprint stripes, but not the structure of their ends nor of their branching and discontinuous defects. The complete model of a loop-free and singularity-free polar domain is given

in figure 8. The polar ends are dominated by a twist of 90° with a helical axis parallel to the domain axis. The twist sense at the round end of the domains is the same as that in the free cholesteric; the twist at the

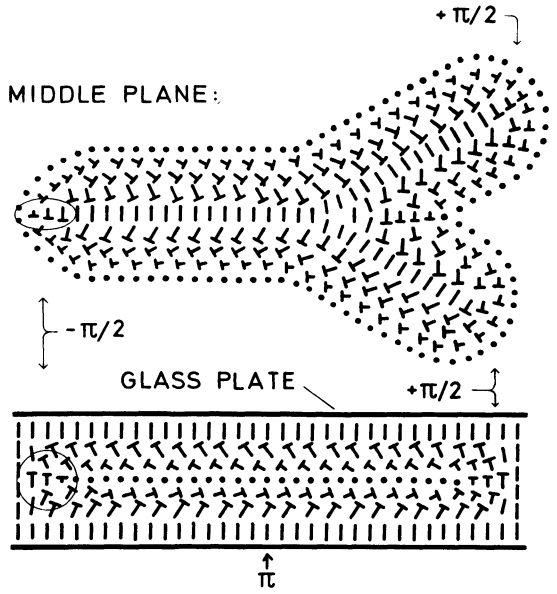

Fig. 8. — Cross sections of a polar cholesteric domain in the elongated and branched state with a maximum midplane tilt angle of 90°. The main part of the structure consists of a conical twist deformation with varying axis. The area with a twist sense opposite to the helical sense of the free cholesteric liquid crystal is encircled. Continuous branching without a director field singularity is only possible to the side of the round end with the proper cholesteric twist.

deformed end is of opposite sense, and has therefore a high density of elastic free energy. This opposite twist, inevitable in the polar domains, is then restricted to a volume as small as possible. If two opposite polar ends approach each other, their twists of opposite senses can annihilate with each other leaving back a continuously merged domain (see Fig. 2). The reverse process of intersecting a domain stripe and generating two polar ends can be initiated by a strong electric field acting inhomogeneously on the domain stripe. The branching of the domain (see Fig. 8) is continuous in contrast to the corresponding τ^+ structure described by Cladis and Kléman [7].

4. **Structure of the spherulitic domains.** — According to the observations, the structure of the spherulitic domains must be in its outer parts identical with that of the round ends of the domain stripes. The centre of the spherulites is dominated by the vertical defect line. The symmetry of the black bands of the spherulite is different from that of a circular loop domain. According to the behaviour in the electric field, the bubble domains must be able to grow from the homeotropic layer by a continuous process and to disappear again without leaving back a singularity. The hysteresis effects show that an energetical barrier between the homeotropic and the spherulitic state is existing. At last, enough splay and bend deformation energy must be cancelled by the equivalent twist deformation where areas with a twist opposite to the free cholesteric must be avoided if possible.

These conditions are fulfilled by the model given in figure 9*a*. The main part of the structure of a spherulitic bubble domain consists of a conical twist with an axis perpendicular to the glass plates. Towards the outer parts of the domain this axis is gradually tilted into a horizontal direction. The density of the bend elastic energy is increasing towards the centre of the domain. There a bend singularity is necessary, because areas of reverse twist are to be avoided and because vertical alignment is not found in the centre, as it is in the loop domains. The proposed model has the required rotational symmetry about the central vertical

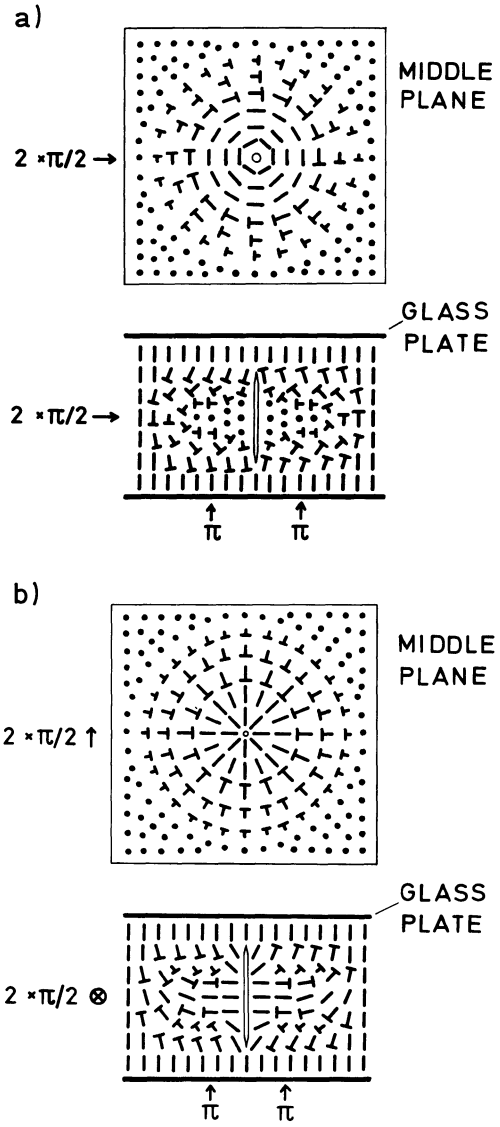

Fig. 9. — Structure of spherulitic domains with a vertical defect line in the centre. *a*) Metastable state with a conical twist of equilibrium pitch. The changing cone aperture gives rise to a twist component with a horizontal axis at the outer edge of the spherulite; *b*) Unstable transition state after the twist-bend transformation by a 90° director turn about the homeotropic axis. The splay singularity can relax by a growth of the conical splay at its ends, and a loop domain as in figure 6 is received.

axis and no mirror plane. The twist has everywhere the same sense as the free cholesteric and the pitch can nearly adopt its equilibrium value.

Since the observed defect line in the centre of the bubble can disappear by a continuous process within a limited volume, it must be topologically unstable and be of the homotopy class 0 [17]. Its relative stability can therefore only be due to a low potential barrier of nontopological character. The intermediate barrier state of this model with a maximum of the elastic free energy is sketched in figure 9*b*. It is generated from the structure in figure 9*a* by the *twist-bend transformation*, where the director in each point is rotated through a constant angle of 90° about the axis of the undisturbed homeotropic alignment [18]. In this special case, the transformation process is also converting bend into splay, and a splay singularity is received in the centre of the domain. The small energy maximum results from the increase of splay-bend deformation at the cost of equilibrium twist in the outer parts, which is only partly compensated by the bend-splay transformation in the centre ($K_1 < K_3$). This energy barrier is then the explanation for the observed hysteresis effect.

The unstable barrier state of figure 9*b* can be transformed into the homeotropic state by the following continuous process : the splay singularity in the centre (see lower part of figure 9*b*) is relaxed to the homeotropic alignment *via* a growth of the rudimentary conical splay at the glass plates. The deformed area left around the homeotropic centre has now a similar structure as the circular loop domain and can unbend and untwist synchronously in the same continuous way to a completely homeotropic alignment. From a topological point of view, the reverse process is possible, but experiments with a decreasing electric field at the homeotropic layer have shown that in the absence of nucleation sites at first a homogeneous conical deformation occurs, which then slowly transforms to parallel stripe domains of the polar type. On the other hand, spherulitic domains can again be received if a high electric field is applied to the homogeneous conical state, before the polar domains have redeveloped.

5. **Discussion.** — The principle of elastic free energy gain by the cholesteric domains in comparison to the homeotropic state is the partial *bend-twist transformation* of the primary deformation, which under these boundary conditions is necessarily of the splay-bend type. In cholesteric liquid crystals this principle is more effective than in nematic liquid crystals, since not only the elastic constant for twist is smaller than that for bend, but because additionally the twisted state can be close to the equilibrium state of the cholesteric.

The distribution of the midplane tilt angle α_m across a domain stripe is controlled by the relative magnitude of the elastic constants and by the ratio of the pitch p_0 *versus* layer thickness d. In this work we have investigated only one liquid crystal mixture and have found nearly a sinus function for α_m with a maximum of 130°. The integral function (5) can describe the double refraction curves of different specimens if the fit parameters a and α_{mm} are varied. The power a of the sinus controls the slope of the function $\Delta\varphi$ at the sides, and α_{mm} the relative depth of the central depression. More detailed investigations have still to be carried out in order to evaluate the influence of the material and layer parameters on the midplane tilt angle of the domains.

The maximum midplane tilt angle α_{mm} is of importance, when an electric field is applied ($\Delta\varepsilon > 0$). For $\alpha_{mm} < 90°$, the domain becomes narrower and disappears as a whole. For $\alpha_{mm} > 90°$, the overtilt is increased by the field [19]. The domain becomes narrower [20], but it can only disappear slowly by shrinking from the ends.

The structure of the defect lines in the centre of the spherulites resembles the Frank disclinations [1] of positive strength. One can speculate, whether the defect lines in the spherulites could have a structure similar to the negative Frank disclinations. In this case one had alternating splay and bend deformations around the vertical line in the centre. The transformation by the rotation of the director about the vertical axis leads only to an interchange of splay and bend, and no basically different structure in received. In contrast to the spherulites with positive defect lines, no relative minimum of the elastic free energy seems to be existing. A continuous generation process for these hypothetical spherulites could not be found. The theoretical considerations are supported by the fact that in the experiments only such spherulites have been observed where the black brushes in polarized light are rotating in the same sense as the polarizer, and not in the opposite sense as it would be the case for the negative spherulites.

In the model, given by Nawa and Nakamura (see Fig. 3*a* in [14]), each sideward extension of a spherulitic domain requires two additional vertical singular lines. This was not observed experimentally and is not needed in the model proposed here. On the other hand, no defect lines parallel to the glass surfaces have been taken into account in the above model, so that it is only compatible with negligible boundary anchoring. The central defect line in our model of the spherulites could be called a *metasingularity* because of its metastable structure. Another model of the spherulites has been considered by Saupe ([2]). In this model the outer parts of the spherulitic domain are the same as in our model. In the midplane of the domain the director is supposed to rotate through a complete turn about the radial axes, which requires defect structures above and below the centre of the domain.

([2]) Private communication by A. Saupe (Kent, Ohio).

These two defect structures, however, have not been observed in experiment.

6. **Conclusion.** — In this work several new experimental observations about the character of the domains in cholesteric layers with homeotropic boundary alignment have been made. Three different types of the fingerprint and spherulitic domains could be distinguished. The models of their structure are respecting both, the homeotropic boundary alignment and the smooth structure of the domains with the exception of the central defect line in the spherulites. The double refraction distribution across a domain with its characteristic depression in the centre could be explained by an overtilting of the director in the centre of the domain. The topological character of the vertical defect line in the centre of the spherulitic domains could be detected as well as the cause for its metastable character.

These results are the basis for a more detailed investigation of layers with a larger relative thickness d/p_0. Then the effects are more complicated because of their multiple superposition, but the structural elements are expected to be the same. In a thick layer with an electric field, reinforcing the homeotropic alignment, the conditions and therefore the observed structures are again rather similar to those in thin layers. Nevertheless there are differences between the static domains and the domains in electric fields, which are yet to be investigated.

It is hoped that the increased understanding of the complicated microstructures in cholesteric layers will support the further efforts to improve the dynamical and optical properties of the dichroic cholesteric display cells.

References

[1] FRANK, F. C., *Discuss. Faraday Soc.* **25** (1958) 19.
[2] FISCHER, F., *Z. Naturforsch.* **31a** (1976) 41.
[3] RAULT, I. and CLADIS, P. E., *Mol. Cryst. Liq. Cryst.* **15** (1971) 1.
[4] HAAS, W. E.L. and ADAMS, J. E., *Appl. Phys. Lett.* **25** (1974) 535.
[5] HAAS, W. E. L. and ADAMS, J. E., *Appl. Phys. Lett.* **25** (1974) 263.
[6] KAWACHI, M., KOGURE, O. and KATO, Y., *Jpn. J. Appl. Phys.* **13** (1974) 1457.
[7] CLADIS, P. E. and KLÉMAN, M., *Mol. Cryst. Liq. Cryst.* **16** (1972) 1.
[8] KASHNOW, R. A., BIGELOV, J. E., COLE, H. S., STEIN, C. R., *Liquid Crystals and Ordered Fluids* **2** (1974) 483.
[9] AKAHANE, T. and TAKO, T., *Mol. Cryst. Liq. Cryst.* **38** (1977) 251.
[10] BHIDE, V. G., CHANDRA, S., JAIN, S. C. and MEDHEKAR, R. K., *J. Appl. Phys.* **47** (1976) 120.
[11] PRESS, M. J. and ARROTT, A. S., *J. Physique* **37** (1976) 387.
[12] STIEB, A. E. and LABES, M. M., *Abstr. VI. Int. Liq. Cryst. Conf.*, Kent, Ohio (1976).
[13] WAHL, J., *J. Physique Colloq.* **40** (1979) C3-98.
[14] NAWA, N. and NAKAMURA, K., *Jpn. J. Appl. Phys.* **17** (1978) 219.
[15] AKAHANE, T., NAKAO, M. and TAKO, T., *Jpn. J. Appl. Phys.* **16** (1977) 241.
[16] MAUGUIN, C., *Bull. Soc. Fr. Minéral.* **34** (1911) 71.
[17] VOLOVIK, G. E. and MINEEV, V. P., *Sov. Phys. JETP* **45** (1977) 1186.
[18] STIEB, A. E. and LABES, M. M., *Mol. Cryst. Liq. Cryst.* **45** (1978) 21.
[19] PRESS, M. J. and ARROTT, A. S., *Mol. Cryst. Liq. Cryst.* **37** (1976) 81.
[20] YU, L. J. and LABES, M. M., *Mol. Cryst. Liq. Cryst.* **28** (1974) 423.